11th ANKARA INTERNATIONAL AEROSPACE CONFERENCE **AIAC-2021-163**

8-10 September 2021 - METU, Ankara TURKEY

AN ALGORITHM FOR WIND TURBINE PROTECTION UNDER ICED ROTOR BLADES

Mustafa Sahin[1] İlkay Yavrucuk[2]

Middle East Technical University
Ankara, Turkey

ABSTRACT

Icing occurs on wind turbines and reduces the turbine aerodynamic performance by changing the blade shapes. It decreases the lift, increases the drag, and thereby the turbine thrust force. In this study, an adaptive algorithm for wind turbine protection is proposed and simulated by the MS Bladed Wind Turbine Simulation Model. The performance of the protection algorithm is tested by simulations for the NREL 5 MW wind turbine with iced rotor blades. The simulation results have shown that the proposed protection algorithm can effectually adapt to the changing turbine operational conditions, i.e., icing, and effectively protect the turbine from having large thrust forces throughout all the operational regions.

Keywords: Turbine Protection, Rotor Blade Icing, Neural Network, Load Alleviation

INTRODUCTION

Wind turbines are commonly used machines to produce electrical energy in the world. More than 90 countries use wind turbines for their electrical demand. Nowadays, the total worldwide installed capacity has exceeded 740 GW according to the last GWEC report. For wind farm installations, on-shore applications are frequently seen, but off-shore applications are gaining popularity in the last decade(GWEC, 2021). Cold and high-altitude areas are also utilized for wind farm installations since they have large wind energy potential due to high-density cold weather and high wind speed. However, icing commonly occurs on the turbines at these wind farms located at high altitudes or near mountains in cold weather. It reduces the turbines' aerodynamic performance and thereby the turbines' power outputs because it changes the shape of rotor blade airfoils. Furthermore, it increases turbines' thrust forces that severely affect turbine components such as blades, tower, gearbox, etc. It also causes structural fatigue, measurement errors, safety hazards, electrical and mechanical component failures, etc.(Brandrud & Krøgenes, 2017) Therefore, the wind power industry uses active and passive methods to get rid of the icing phenomenon. In passive methods, turbine blades are painted in black, stick-free surface, or

[1] Dr. Instructor, METU Center for Wind Energy, e-mail: musahin@metu.edu.tr

[2] Associate Professor, Department of Aerospace Engineering, e-mail: yavrucuk@metu.edu.tr

special materials are used for coatings. In active methods, however, an electrical ice protection system using hot air circulation inside the blade is a widely-used strategy. A thermal system that applies heating to the blades is also another technique(Baring-Gould et al., 2010).

In this study, a protection algorithm is proposed to protect turbines with iced blades from the above issues such as component failures due to excessive thrust force. This study is an extension of our previous work on the Adaptive Envelope Protection (EPS) System presented at ICWEEA 2020 and published in Ref(Sahin & Yavrucuk, 2020). In that study, the adaptive EPS algorithm is tested only under the changes in turbine operating point for the below and above rated region of wind turbines, i.e., Region II and III. Here, the EPS algorithm is expanded to protect turbines under icing conditions, i.e., iced turbine blades.

The proposed algorithm monitors wind and turbine states in real-time, and adapts itself to rotor blade icing, and takes a protection action whenever required, namely, before the thrust force of a turbine exceeding a pre-defined thrust limit value. The protection action is realized by interacting with the blade pitch control system output, and changing the blade pitch reference, thereby the blade pitch angles, collectively. Here, the simulations of the EPS algorithm are realized for the NREL 5 MW turbine with iced blades. Simulations show that the proposed EPS algorithm adapts itself to the changes/icing on the 5 MW turbine and continues to keep the turbine within safe operational limits, i.e., a pre-defined thrust limit. Thus, it protects the turbine from damages.

This paper is organized as follows. Section 2 shortly defines the MS Bladed Wind Turbine Simulation Model and Baseline Controllers for NREL 5 MW turbine. Section 3 focuses on the theory of the adaptive EPS algorithm. Section 4 is about the implementation of the EPS algorithm on the NREL 5 MW turbine for limiting the thrust force. Section 5 briefly explains blade icing and its modeling for the NREL 5 MW turbine. Section 6 includes the simulation results and concludes the study.

THE MS BLADED WIND TURBINE MODEL and BASELINE TURBINE CONTROLS

The MS (Mustafa Sahin) Bladed Model, which is based on Blade Element Momentum (BEM) theory, is developed for Horizontal Axis Wind Turbine simulations. The aerodynamic calculations within the MS Bladed Model are similar to those of Prop Code(Wilson & Lissaman, 1974), Wt_Perf(Platt & Buhl, 2012), and Aerodyn(Moriarty & Hansen, 2005). The model employs various particular coordinate systems and important aerodynamic corrections. It has the capabilities of nacelle yawing and individual or collective blade pitching. It allows the users to define desired rotor pre-cone and nacelle tilt angles. The MS Bladed Model includes a turbine rotor, a gearbox, and a simple variable torque electrical generator. The current version of the MS Bladed Model considers all the turbine parts such as blades, shafts, etc. as rigid structures. More information about the MS Bladed Model may be found in Ref(Sahin, 2018; Sahin & Yavrucuk, 2017a, 2017c).

Inside the MS Bladed Model, the properties of the NREL 5 MW wind turbine(Jonkman, Butterfield, Musial, & Scott, 2009) are used. Baseline generator torque and collective blade pitch controllers are designed, accordingly(Sahin & Yavrucuk, 2019b, 2019a, 2017b). In Region II, a nonlinear generator torque controller is employed for maximum power production, whereas, in Region III, a collective blade pitch controller is used for regulating the turbine power output to the rated power. Rate limiters and saturation limits are added to the outputs of the baseline controllers. The blade pitch actuator dynamics is included, while the torque actuator dynamics is neglected. Also, two transition region torque controllers such as Region $I^{1/2}$ and Region $II^{1/2}$ are added to the baseline control systems: one between Region I and II, one between Region II and Region III. Transitions from Region I to Region II and Region II to Region III are carried out dynamically by these transition region torque controllers based on rotor speed information.

THE ADAPTIVE ENVELOPE PROTECTION SYSTEM (EPS) ALGORITHM

In the proposed EPS algorithm, any parameter, which is desired to be limited on the turbine, is referred to as a limit parameter. Also, turbine states are considered to consist of fast and slow states. The limit parameter dynamics is driven by the fast and slow states as well as the input. Thus, a limit parameter dynamics can be written as,

$$\dot{y}_l = r(x_s, x_f, u) \tag{1}$$

Here, it is thought that the limit parameter dynamics is affected largely by the fast states. Therefore, the limit parameter dynamics is written as

$$\dot{y}_l = \tilde{r}(y_l, x_s, u) \tag{2}$$

where y_l represents the limit parameter, x_s is the slow state, u is the input to the turbine system. In the proposed EPS algorithm, an approximate model is used to estimate the nonlinear dynamics of the limit parameter. Therefore, an approximate model in (3) is selected for the limit parameter. In this study, as a limit parameter, the thrust force is chosen since it is a vital load on turbine components, and particularly increases with ice accumulation.

$$\dot{\hat{y}}_l = A\hat{y}_l + Bu \tag{3}$$

The approximate model in (3) cannot capture the nonlinear dynamics of the limit parameter of an actual turbine system because there is usually a modeling error, ξ as in (4).

$$\dot{y}_l = A\hat{y}_l + Bu + \xi(y_l, x_s, u) \tag{4}$$

Therefore, it is augmented here with a neural network along with an observer as follows(Yavrucuk & Prasad, 2012).

$$\dot{\hat{y}}_l = A\hat{y}_l + Bu + \Delta(y_l, x_s, u) + K(y_l - \hat{y}_l) \tag{5}$$

where Δ is the neural network (LPNN) output and *K* is the observer gain matrix, while $y_l - \hat{y}_l$ is the error, e. Δ is defined as

$$\Delta = W^T \delta(\mu) \tag{6}$$

where W, δ, μ represent the network weights, basis functions, input vector, respectively. If the augmented model (5) is subtracted from (4), error dynamics in (7) is obtained. For a Hurtwitz K matrix, e goes to zero if the modeling error, ξ is canceled by the neural network output, Δ. Then, the adaptation is satisfied.

$$\dot{e} = \xi - \Delta - Ke \tag{7}$$

Thus, the augmented model and the actual nonlinear turbine system produces almost the same limit parameter output in time, i.e, $\hat{y}_l = y_l$. This is obtained by estimating the limit parameter dynamics online (Figure 1). The neural network weight update law is given as(Yavrucuk & Prasad, 2012).

$$\dot{\hat{W}} = \Gamma\left(\delta e^T P - k\hat{W}\|e\|\right) \tag{8}$$

where k is the gain of e-modification term, Γ is the learning rate of the neural network, and *P* is the solution of the Lyapunov equation below.

$$(-K)^T P + P(-K) = -I \tag{9}$$

δ is defined as follows.

$$\delta(y_l, x_s, u) = D_1 \oplus D_2 \tag{10}$$

Where $\oplus$ is the Kronecker product, D_1 and D_2 are the following vectors with 1s as bias terms.

$$D_1 = [1\ y_l\ x_s] \tag{11}$$

$$D_2 = [1\ u] \tag{12}$$

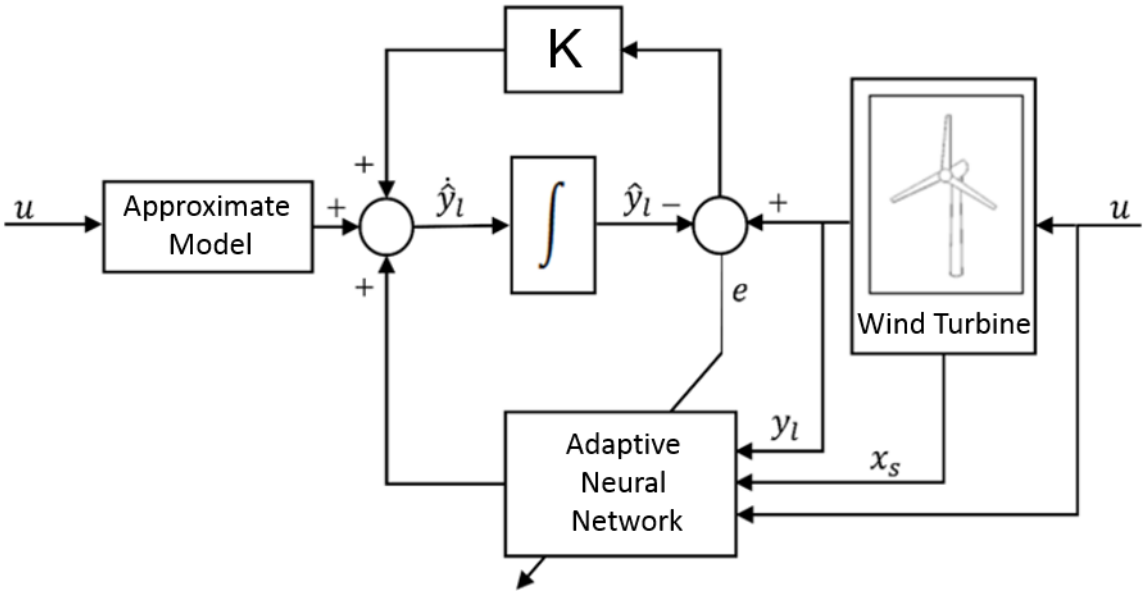

Figure 1 Online estimation of limit parameter dynamics(Sahin & Yavrucuk, 2020)

Also, an envelope wind speed, u_{env}, which takes the turbine to the pre-defined/desired envelope limit, y_{l_d} is calculated from (13) through a fixed point iteration during online estimation of limit parameter dynamics (Figure 1).

$$u_{env} = -B^{-1}\left(Ay_{l_d} + \Delta(y_l, x_s, u) + Ke - \dot{\hat{y}}_l\right) \tag{13}$$

Later, by the formulation (14), envelope wind speed is compared with the actual wind speed to determine if the turbine operates with the excessive load or not, i.e., high thrust force or not.

$$\Delta u = u_{env} - u \tag{14}$$

A positive Δu means that the turbine operates within a safe operational thrust limit value, whereas a negative Δu corresponds to the situation of excessive thrust force. This information, Δu is later used to determine the amount of blade pitch angle reference, $\Delta\beta_{ref}$ and thereby the blade pitch angle, β to be required for protecting the turbine. The relation (15) is defined between, $\Delta\beta_{ref}$, and Δu.

$$\Delta\beta_{ref} = \varepsilon\Delta u \tag{15}$$

where ε is a design parameter. In this study, the same design parameters and values in Ref(Sahin & Yavrucuk, 2020) are used for the proposed adaptive EPS algorithm. Note that all above calculations are realized in real-time and the algorithm adapts to the current turbine operations and produces an avoidance signal, $\Delta\beta_{ref}$ only if the EPS system is on and the turbine is about to exceed the pre-defined safe limit.

ALGORITHM IMPLEMENTATION TO LIMIT THE TURBINE THRUST FORCE

Here, the proposed adaptive EPS algorithm estimates the limit parameter dynamics online and calculates the envelope wind input that takes the turbine to the desired thrust limit through an iteration and decides whether the turbine operates with the excessive thrust force or not, and accordingly produces an avoidance signal when required.

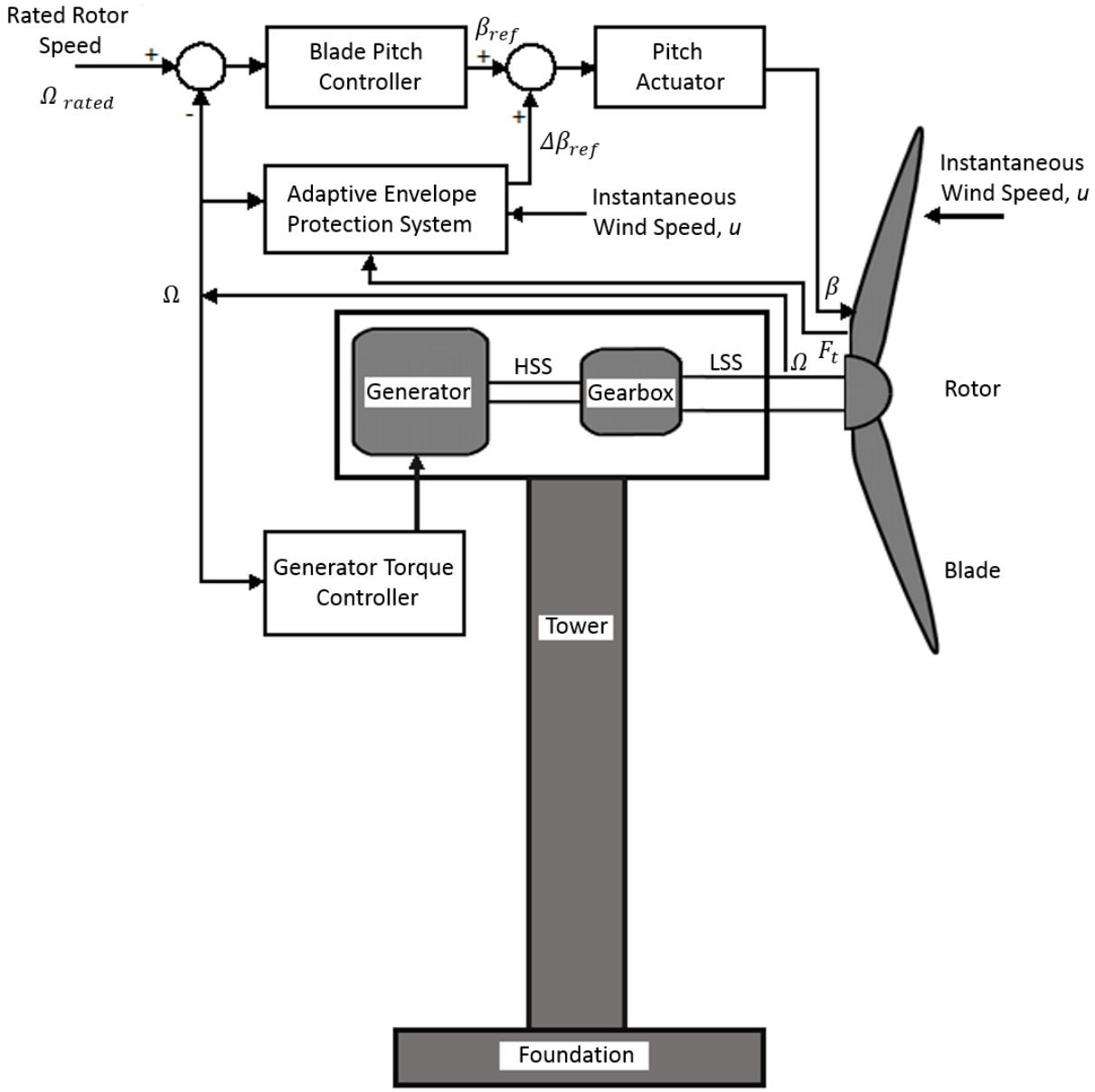

Figure 2 A wind turbine with baseline controllers and the adaptive EPS algorithm

Figure 2 generally shows the algorithm implementation on a turbine with baseline controllers. As seen from the figure, wind and turbine states such as turbine rotor speed, Ω, thrust force, F_t and wind speed,u are monitored by the adaptive EPS algorithm through an adaptive neural network(Figure 1). Based on these data, an extra blade pitch reference signal that is to be added to the output of the blade pitch controller is generated when necessary.

In algorithm implementation, the approximate model is written for the thrust force as follows.

$$\dot{\hat{F}}_t = \mathrm{a}\hat{F}_t + \mathrm{b}u \tag{16}$$

Where a and b are the approximate values and u is the actual wind input. Then, the augmented model becomes as

$$\dot{\hat{F}}_t = \mathrm{a}\hat{F}_t + \mathrm{b}u + \Delta(F_t, \Omega, u) + K(F_t - \hat{F}_t) \tag{17}$$

and $D_1$and D_2 vectors are chosen as

$$D_1 = [1\ F_t\ \Omega] \tag{18}$$

$$D_2 = [1\ u] \tag{19}$$

The envelope wind speed, u_{env}, is calculated for the desired/pre-defined thrust limit, F_{t_d} as

$$u_{env} = -b^{-1}\left(aF_{t_d} + \Delta(F_t, \Omega, u) + Ke - \dot{\hat{F}}_t\right) \tag{20}$$

ROTOR BLADE ICING MODELING

When investigated the literature, there are numerical and experimental studies on wind turbine blade icing(Brandrud & Krøgenes, 2017; Hu, Zhu, Chen, Shen, & Du, 2018; Jin & Virk, 2020; Yirtici, Ozgen, & Tuncer, 2019; Yirtici, Sevine, Ozgen, & Tuncer, 2018). For icing modeling on the NREL 5 MW turbine blades, this study is inspired by the experimental aerodynamic investigation of Brandrud and Krøgenes on blade icing. They examined the effects of icing on the aerodynamics of a wind turbine blade such as the NREL S826 airfoil(Brandrud & Krøgenes, 2017) both experimentally and computationally.

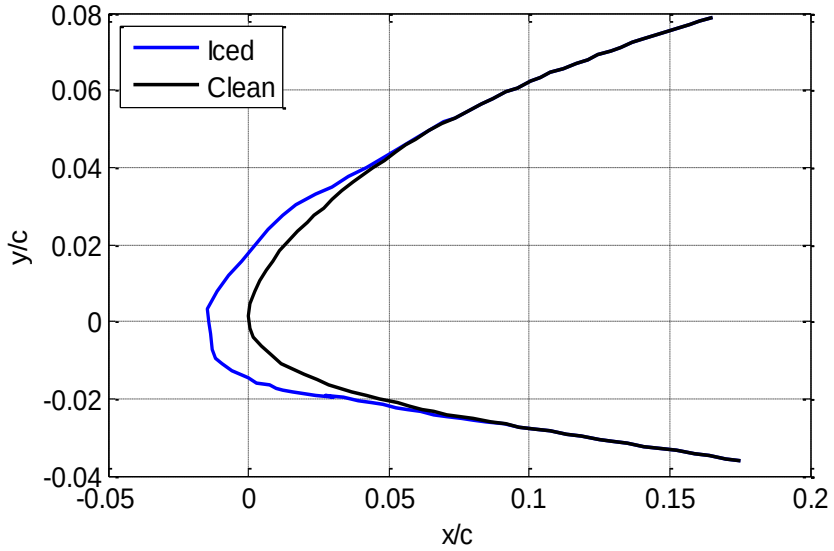

Figure 3 Glaze Icing on the leading edge of the NREL S826 airfoil(Brandrud & Krøgenes, 2017)

In their investigations, three different ice accretion types; glaze, rime, and mixed icing are studied with artificial ice shapes attached to the leading edge of the S826 airfoil. 2D ice shapes are

generated using the LEWICE code (version 3.2.2)(Wright, 2008). It is also declared that the utilized ice shapes may not fully represent each icing type since ice shapes depend on various parameters such as freestream icing velocity, ambient temperature, liquid water content, median volume diameter, icing duration, angle of attack, airfoil chord length. For all the three types of ice accretions, the lift is decreased, while drag is increased with respect to the clean airfoil. In the linear lift region, approximately 10-15% lift reduction occurs for the rime and glaze icing cases, 25-30% lift reduction for the mixed ice case. For drag, rime and glaze icing types have similar tendencies, but mixed ice leads to extreme performance deterioration. For example, rime ice causes a 50% increase in drag, whereas mixed ice 600% increase in drag at the normal operation region at around an AOA of 7-degrees. Here, in this study, one of the above icing types, i.e., glaze icing, is considered. The generated shape for the glaze icing is seen in Figure 3 and the defined parameters are given in Table 1(Brandrud & Krøgenes, 2017).

Table 1: Parameters defined for the glaze icing (Brandrud & Krøgenes, 2017)

Freestream Icing Velocity	V_{icing}	25 m/s
Temperature	T	-2 ºC
Liquid Water Content	LWC	0.34 g/m3
Median Volume Diameter	MVD	30 μm
Icing Duration	t_{icing}	40 minutes
Angle of Attack	AOA	1º
Airfoil Chord Length	c	0.3 m

Figure 4 shows the experimental aerodynamic data obtained by Ref(Brandrud & Krøgenes, 2017) for the clean and iced S826 airfoil, i.e., glaze icing in Figure 3. As seen in Figure 4, due to icing, it is clear that lift is reduced, while drag is increased at the same AOAs.

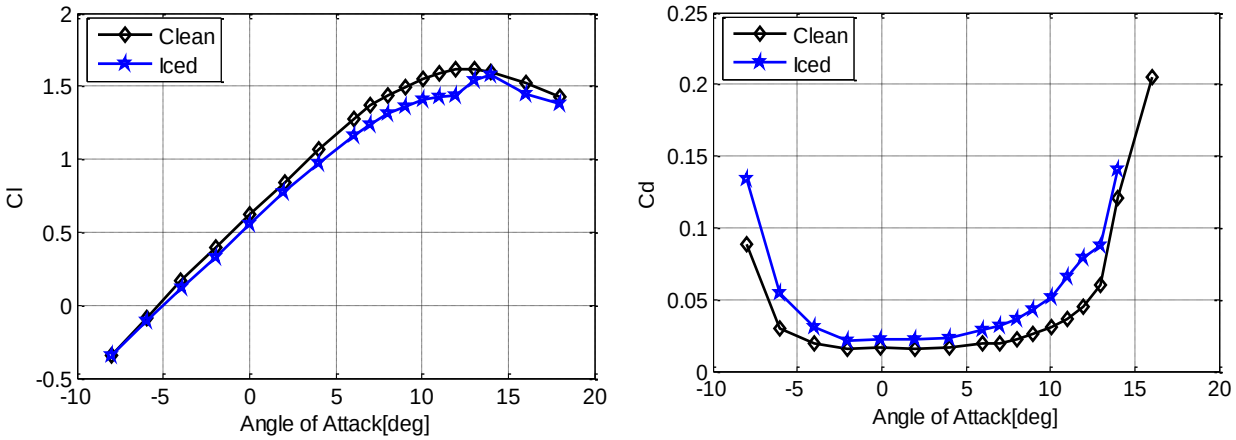

a) b)

Figure 4 The NREL S826 airfoil data at Re=4x10^5, a) Cl data for clean and iced airfoils, b) Cd data for clean and iced airfoils (Brandrud & Krøgenes, 2017)

When the icing phenomenon is considered for a wind turbine blade, along the blade span, ice accretion does not occur uniformly. It increases from the blade root to the tip depending on the blade's angular motion (Salam Alsabagh, 2016). Considering the glaze icing case in Figure 3 and its resulting impacts on the aerodynamic data in Figure 4, icing modeling on the NREL 5 MW

turbine blades is carried out as follows. The aerodynamic data of all NREL 5 MW turbine blade airfoils are modified to imitate icing. Modification in the aerodynamic data is increased towards blade tips. Namely, lift reduction and drag rise are getting dominant from the blades' roots to the tips. The original extrapolated aerodynamic data(Jonkman et al., 2009) of all the NREL 5 MW turbine airfoils are modified and are later used in the MS Bladed Model. For instance, Figure 5 shows the original (C_{l_o}, C_{d_o}) and the modified (C_{l_m}, C_{d_m}) aerodynamic data for DU35A17 and DU21A17 airfoils used respectively at the 6th and 11th sections of the NREL 5 MW turbine blades.

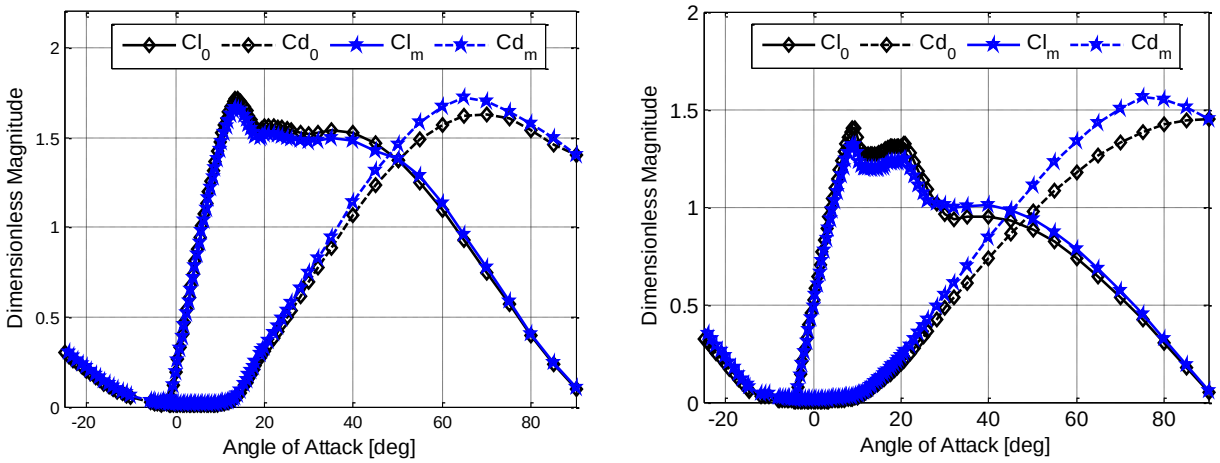

Figure 5 Original and modified aerodynamic data, a) DU35A17, b) DU21A17

The modification in the aerodynamic data for all the 5 MW turbine blade airfoils is realized between AOA of -25 and 90 degrees, such that the lift and drag curves cross each other at around an AOA of 50 degrees. Additionally, the turbine rotor inertia is increased by 3% due to the ice accumulation on the blades.

SIMULATION RESULTS AND CONCLUSIONS

In this section, the MS Bladed Model simulations for the controlled NREL 5 MW turbine with clean and iced rotor blades are presented. Also, simulation with EPS on is evaluated. All the simulations are given for 50 seconds and the thrust limit is defined as 0.55 MN. Figure 6 shows the simulation results of the controlled NREL 5 MW turbine with clean and iced rotor blades under a turbulent wind with a mean of 14 m/s. Figure 6-a, b, and c respectively show the changes in applied wind speed, blade pitch angle, and turbine thrust force in time. The simulation results are given for Region III operation. As you can see, most of the time, the turbine with clean and iced blades produces large thrust forces, which exceed the pre-defined/desired thrust limit of 0.55 MN given in red (Figure 6-c). Except for the initial seconds of the simulation, the controlled NREL 5 MW turbine with iced rotor blades exposes to much higher thrust forces than the case with clean blades. This is due to the ice accumulation on the turbine blades, which changes blades' shapes and decreases the lift, and increases the drag, and thereby the thrust force. At the initial instants of the simulation, the 5 MW turbine with clean, and iced rotor blades operates with the initial conditions and tries to recover its operation to the applied turbulent wind speed(Figure 6-a). That's why clean blades produce larger thrust forces than iced blades at initial seconds.

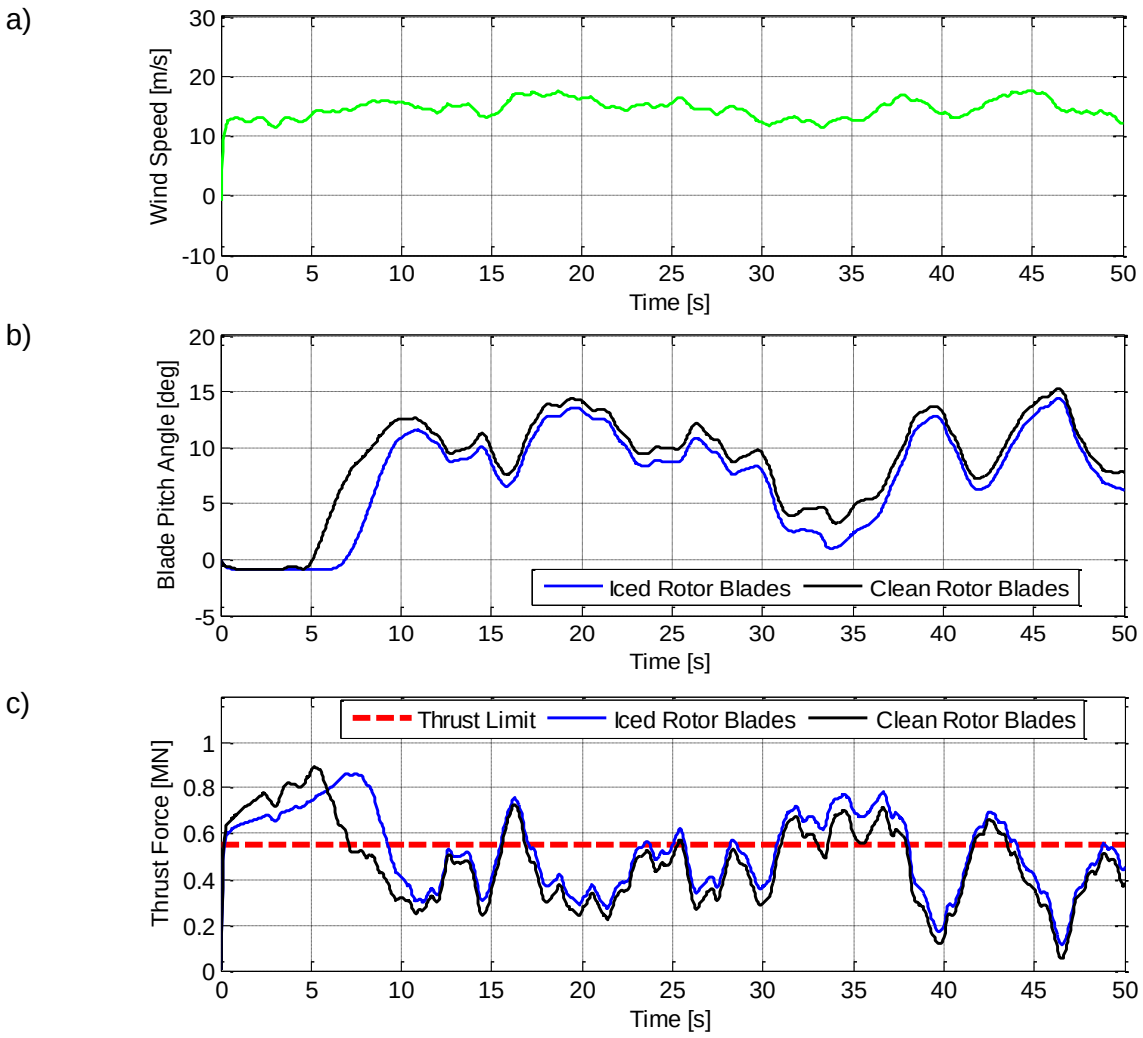

Figure 6 Simulation results of the controlled NREL 5 MW turbine with clean and iced rotor blades

When the blade pitch controller starts changing the blade pitch angles sometime later for power output regulation, iced rotor blades generate larger thrust forces than clean blades. To obtain the same power output in Region III from the iced turbine, the blade pitch controller adjusts blade pitch angles in time to lower values. In both cases, particularly with iced blades, the NREL 5 MW turbine operates with excessive thrust force, which is not a safe turbine operation.

In Ref(Sahin & Yavrucuk, 2020), prevention of excessive thrust force of the NREL 5 MW turbine, i.e., with clean blades, through the adaptive EPS algorithm is investigated for the below and above rated turbine operation regions. Therefore, in this study, the focus is to demonstrate the efficacy of the adaptive EPS algorithm to eliminate the excessive thrust force (Figure 6-c) due to iced blades. Thus, with the next simulation results, whether the proposed adaptive EPS algorithm manages to keep the iced turbine within the pre-defined limit or not is investigated in detail. Extra turbine variables are added to the above simulation in Figure 6, such as envelope wind speed, neural network learning weights, and all are presented in Figure 7. Also, all the variables are given as solid and dashed lines, respectively when the adaptive EPS algorithm is on and off.

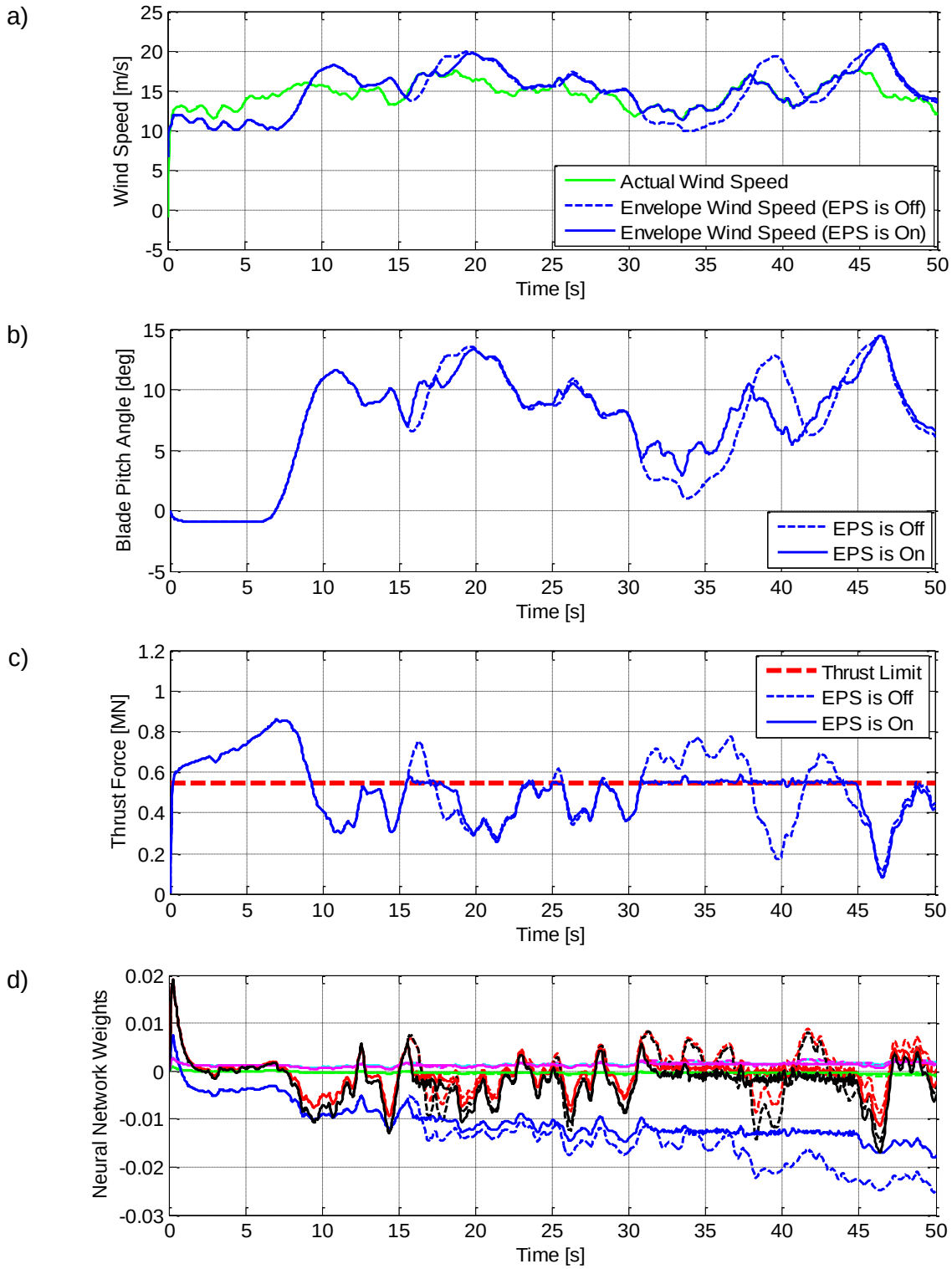

Figure 7 Simulation results for the adaptive EPS algorithm for the NREL 5 MW turbine with iced rotor blades at Region III, a) Actual and envelope wind speed, b) Blade pitch angle, c) Thrust force, d) NN learning weights

As seen from Figure 7-a, when the turbine with iced blades operates with the adaptive EPS system off, most of the time, the actual wind speed becomes larger than the envelope wind speed, which corresponds to a turbine operation with excessive thrust force(Figure 7-c). Here, the adaptive EPS system is not active, but still monitors the wind and turbine states and adapts to icing. When the adaptive EPS system is activated at 10s, using the adaptation through the neural network, the system estimates the near future value for the thrust force in time and takes an avoidance action before the thrust force exceeds the envelope limit. This is realized by generating a blade pitch reference that is applied to the output of the blade pitch controller to vary the blade pitch angle(Figure 7-b). Hence, the algorithm rides the turbine at the thrust limit(Figure -c) and the turbine is kept safe within the desired thrust limit. Figure 7-d shows the changes in NN learning weights when the adaptive EPS is off (dashed) and on (solid).

In this study, the adaptive EPS algorithm in Ref(Sahin & Yavrucuk, 2020) is expanded to protect turbines with iced blades. The proposed EPS algorithm is tested for various turbine operation regions under the case of iced blades, i.e., glaze icing case. In all the simulations, the adaptive envelope protection system manages to keep the turbine within the pre-defined thrust limit. Here, only the Region III simulations are given as an example. From the simulation results, it is concluded that the proposed EPS algorithm adapts to the icing phenomenon on rotor blades and allows a safe turbine operation. Thus, even in icing conditions, which increase turbines' thrust forces, the proposed adaptive EPS algorithm can protect turbines from failures and eventually increases the service life of turbines.

REFERENCES

Baring-Gould, L., Tallhaug, L., Ronsten, G., Horbaty, R., Cattin, R., Laakso, T., … Wallenius, T. (2010). *Recommendations for wind energy projects in cold climates* (VTT Working Papers No. 1459–7683). Finland.

Brandrud, L., & Krøgenes, J. (2017). *Aerodynamic Performance of the NREL S826 Airfoil in Icing Conditions*. Norwegian University of Science and Technology. Retrieved from https://pdfs.semanticscholar.org/c04b/47e6c9e34788aade2f9e6c376c92302c14b1.pdf?_ga=2.201964753.1399202697.1630476771-1528367017.1623846326

GWEC. (2021). GWEC | GLOBAL WIND REPORT 2021.

Hu, L., Zhu, X., Chen, J., Shen, X., & Du, Z. (2018). Numerical simulation of rime ice on NREL Phase VI blade. *Journal of Wind Engineering and Industrial Aerodynamics*, *178*(May), 57–68. https://doi.org/10.1016/j.jweia.2018.05.007

Jin, J. Y., & Virk, M. S. (2020). Experimental study of ice accretion on S826 & S832 wind turbine blade profiles. *Cold Regions Science and Technology*, *169*(July 2019). https://doi.org/10.1016/j.coldregions.2019.102913

Jonkman, J., Butterfield, S., Musial, W., & Scott, G. (2009). *Definition of a 5-MW Reference Wind Turbine for Offshore System Development*. *Technical Report NREL/TP-500-38060*.

Moriarty, P. J., & Hansen, A. C. (2005). *AeroDyn Theory Manual, NREL/TP-500-36881, Golden, Colorado: National Renewable Energy Laboratory*.

Platt, A. D., & Buhl, M. L. (2012). *WT_Perf User Guide for Version 3.05.00*.

Sahin, M. (2018). *Dynamic Modeling, Control and Adaptive Envelope Protection System for Horizontal Axis Wind Turbines, PhD Thesis, Department of Aerospace Engineering, METU, Ankara*. Middle East Technical University.

Sahin, M., & Yavrucuk, I. (2017a). Dynamical modelling of a wind turbine system with precone and tilt angles. In *9th Ankara International Aerospace Conference* (pp. 1–11). Ankara, Turkey.

Sahin, M., & Yavrucuk, I. (2019a). Performance Comparison of Two Turbine Blade Pitch

Controller Design Methods Based on Equilibrium and Frozen Wake Assumptions. In *Ankara International Aerospace Conference, AIAC 2019* (pp. 1–16). Ankara, Turkey.

Sahin, M., & Yavrucuk, I. (2019b). Rüzgar Türbini Kanat Yunuslama Açısı Kontrolcüsü Tasarımı ve Performans Analizi. In *5. İzmir Rüzgâr Sempozyum*. İzmir.

Sahin, M., & Yavrucuk, İ. (2017b). Değişken Hızlı Rüzgar Türbinlerinin Kısmi ve Tam Yük Bölgeleri için Kontrolcü Tasarımı. In *YEKSEM 2017* (p. 12). Antalya.

Sahin, M., & Yavrucuk, İ. (2017c). Rüzgar Türbininin Dinamik Modellemesinde Belirli Parametrelerin Güç Eğrisi Tahminine Olan Etkilerinin İncelenmesi. In *YEKSEM 2017* (p. 8). Antalya.

Sahin, M., & Yavrucuk, İ. (2020). Adaptive Envelope Protection Control for the below and above Rated Regions of Wind Turbines. *World Academy of Science, Engineering and Technology, International Journal of Energy and Power Engineering*, *14*(10), 275–283.

Salam Alsabagh, A. (2016). *Effect of Atmospheric Ice Accretion on the Dynamic Performance of Wind Turbine Blades*. University of Hertfordshire. Retrieved from http://uhra.herts.ac.uk/bitstream/handle/2299/17990/14087025 Alsabagh Abdel final PhD submission.pdf?sequence=1

Wilson, R. E., & Lissaman, P. B. S. (1974). *Applied Aerodynamics of Wind Power Machines*.

Wright, W. (2008). User's Manual for LEWICE Version 3.2. *NASA/CR-2008-214255*, (November).

Yavrucuk, I., & Prasad, J. V. R. (2012). Online Dynamic Trim and Control Limit Estimation. *Journal of Guidance, Control, and Dynamics*, *35*(5), 1647–1656. https://doi.org/10.2514/1.53116

Yirtici, O., Ozgen, S., & Tuncer, I. H. (2019). Predictions of ice formations on wind turbine blades and power production losses due to icing. *Wind Energy*, *22*(7), 945–958. https://doi.org/10.1002/we.2333

Yirtici, O., Sevine, T., Ozgen, S., & Tuncer, I. H. (2018). Wind turbine power production losses due to ice accretion on turbine blades. *2018 Joint Thermophysics and Heat Transfer Conference*, 1–12. https://doi.org/10.2514/6.2018-4291